IEEE Access
Multidisciplinary | Rapid Review | Open Access Journal

Received August 29, 2021, accepted September 15, 2021, date of publication September 17, 2021,
date of current version September 27, 2021.

Digital Object Identifier 10.1109/ACCESS.2021.3113733

Effective Modeling of OUPFC Into Newton-Raphson Power Flow Considering Multi-Control Modes and Operating Constraints

MOHAMED EBEED HUSSEIN[1], FATMA RABEA[2], SALAH KAMEL[2], AND EYAD S. ODA[3], (Member, IEEE)

[1]Department of Electrical Engineering, Faculty of Engineering, Sohag University, Sohag 82524, Egypt
[2]Department of Electrical Engineering, Faculty of Engineering, Aswan University, Aswan 81542, Egypt
[3]Department of Electrical Engineering, Faculty of Engineering, Suez Canal University, Ismailia 41522, Egypt

Corresponding author: Eyad S. Oda (eyad.oda@eng.suez.edu.eg)

ABSTRACT The Optimal Unified Power Flow Controller (OUPFC) is an efficient series-shunt controller that is incorporated to system to control the power flow through the transmission lines. Modeling of such controller is a challenge task due the required complex modifications of the Newton Raphson power (NR) flow to consider the parameters of the OUPFC. The aim of this paper includes (1) presenting an efficient novel model of the OUPFC into NR power flow, (2) avoiding the complicities of modeling the parameters of the OUPFC into power flow solution, (3) multi-control modes of the OUPFC is established to control the active and reactive powers concurrently or separately and, (4) handling the violation of the operating constraints by using developed methods. The proposed model is based on the power injection representation where the parameters of the OUPFC are represented as injected loads as a function of the pre-requested control variables (specified values). Therefore, the complicities of including its parameters are reduced. The developed methods for handling the violations of the operating constraints are based on modifying the specified values as a function of the maximum limits of the operating constraints. The proposed OUPFC model and the developed constraints handling methods are implemented on IEEE 14-bus, IEEE 30-bus, IEEE 57-bus and IEEE 118-bus test systems. The simulation results verified the feasibilityand robustness of the presented model into load flow analysis. in addition, effectiveness of the proposed approaches forhandling the operating constraints of OUPFC.

INDEX TERMS Power flow, FACTS, optimal unified power flow controller, the operating constraints.

NOMENCLATURE

I_{inj}	The injected current to sending bus.
I_{sp}	The specified current passing through transmission line.
I_{sh}	The shunt current.
I_{jr}	The current between bus j & receiving bus r.
I_{se}^{max}	The maximum series current.
V_{inj}	The injected voltage.
V_{inj}^{max}	The maximum injected voltage.
V_s	The voltage of the sending bus.
V_j	The voltage at bus j.
V_r	Receiving voltage.
Z_s	The series impedance of the OUPFC.
Z_{Line}	The series impedance of the TL.
S_{sp}	The specified apparent power in the TL.
P_{sp}	The specified active power in the TL.
Q_{sp}	The specified reactive power in the TL.
S_{sh}	The shunt apparent power.
S_s	The injected apparent power at sending bus s.
S_j	The injected apparent power at bus j.
Q_{jr}	The reactive power between bus j & receiving bus r.
P_{jr}	The active power between bus j & receiving bus r.
Re	Superscript refers to the real part.
Im	Superscript refers to the imaginary part.

The associate editor coordinating the review of this manuscript and approving it for publication was Hazlie Mokhlis.

I. INTRODUCTION

A. LITERATURE SURVEY

The Flexible Alternating Current Transmission System (FACTS) has become the head of concern of the modern

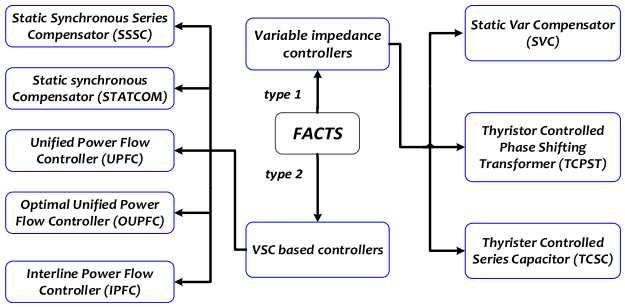

FIGURE 1. Types of FACTS controllers based on the power electronic devices.

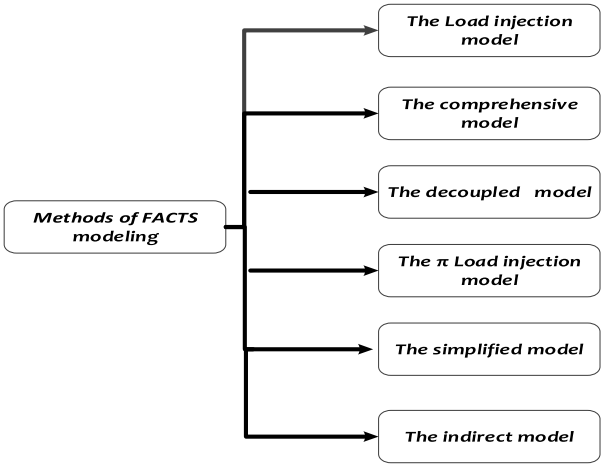

FIGURE 2. Methods of modeling FACTS device.

powers where the FACTS can change the parameters of the power system such as the transmission line impedance, the magnitude and the phase angle of the buses voltage and the power flow in the network. Consequently, the FACTS are widely used to enhancing the technical and economic issues related to the power system operation including enhancing the system stability, the loadability, the security, minimizing the power losses and system generation cost [1], [2].

The FACTS controllers are power electronic devices, from this prospective FACTS can be classified into two types as depicted in Figure 1: (1) The variable impedance type and (2) The Voltage Source Converter (VSC) type [3]. It should be point out here that the FACTS controllers based VSC have high control ability compared with the variable impedance FACTS where the FACTS controllers based VSC can inject AC voltage with controllable voltage magnitude and phase angles to system. Thus, this VSC based type can control the power flow efficiently.

Modeling of the FACTS devices into Newton Raphson power flow solution requires several modifications are to represent these devices. For modelling, the first type (variable impedance modification), numerous modifications are required in the line data, bus data and the Y-bus while modeling the second types (VSC based controller) needs difficult modifications in Jacobian, corrections, power mismatches matrices of the Newton Raphson (NR). The required modifications are applied to consider the contributions of the series and shunt voltage sources of the controllers [4]–[6].

Several efforts have been presented for modelling the VSC based controllers which are depicted in Figure 2. The load injection model was presented in [7]. In this model the controller is represented as injected active and reactive powers at its terminal buses which are driven from the voltage source representation of the controller. A modification of Jacobian matrix is required to incorporate the active and reactive powers. The π Load injection model was presented in [8], in this model the controller is represented by a π equivalent circuit with injected loads at its terminals. The disadvantage of this model is that numerous equations are embedded into the power flow solution to represent the controller. In addition of that the transmission line and the controller resistances are neglected. The decoupled model was presented in [9], [10], to represent the controllers by this method, the send end and the received end buses are separated. Then, the sending end bus is represented as a PV bus while the receiving end is represented as a PQ bus. The model is an effective model but a set of modifications in Jacobean matrix are required related to parameters of the controller. The simplified model was proposed in [11], in this model the controller is represented as fictitious loads which are updated as a function of specified values. The model is an efficient model, and no changes are required in Jacobian matrix. However, the operating constraints of the controller are not considered. The convergence of the power flow solution with the simplified model was obtained after 40 iterations. References [12] and [13] propose a comprehensive model of the UPFC in Newton Raphson power flow. The merit of this model is that it is a multi-control model where the UPFC can control the active and reactive powers as well as the voltage magnitude concurrently. In addition of that the losses of UPFC are considered in solution of the power flow. However, the shortage of this model is that a set of equations are implemented in the power flow to represents the UPFC as well as a modification is required in Jacobian matrix of NR power flow which increases the complicities of representation this controller. The accuracy of the power flow with the comprehensive model is selected to be 10-12 and the convergence was obtained in 7 and 4 for [12] and [13], respectively. The direct model was presented in [14], where the controller is represented by an augmented equivalent network with adding auxiliary load buses. The merits of this model include the symmetry of the original Jacobian matrix are not changed and the constraints are not taken into consideration. However, subsections are included to the basic Jacobian matrix to represents the controller. The accuracy of the power flow with the direct model is 10-12 and convergence was obtained in 7 iterations. The authors in [15]–[18] presented developed models of the controllers which is captured from the power injection representation where the converters are represented as current sources as a function of the specified

or the specified values then the current sources are converted to the power injection loads. The modifications are avoided, and the operating constraints are considered but some controllers are not represented such as the STATACOM, the OUPFC and the hybrid flow controller (HFC). The operating constraints of the FACTS devices are related to the rating of their converters. The operating constraints should be considered with the FACTS modeling to realize their practical capabilities. The constraints of FACTS controller include the current passing via their converters and the injected voltages by the converters as well as the exchanged power via converters. Violation of the operating constraints occurs when their values being more than the allowable limits. Several papers have been provided to enforce or handle the violations of the operating constraints into power flow solution. S. Kamel *et al.* presented an efficient model for Center-node Unified Power Flow Controller into power flow analysis with enforcement its operating constraints including the injected series and shunt voltages, the series and shunt currents passing through the VSCs of the controller and the exchanged power in this controller [19]. In [20], a power injection model of the SSSC with Multi-control Functional has been presented with handling the violations of operating constraints including the series injected voltage of the SSSC and the passing current through this controller. The operating constraints of the UPFC have been enforced in [21] including the series and the shunt injected voltages of the UPFC, the series current passing through the inverter and the exchanged power through the inverters.

The OUPFC is an effective controller which can be incorporated in system to control the power flow in the transmission lines. Few papers have been presented to describe modeling or assigning the optimal location of the OUPFC. The authors in [22] presented a power injection model of the OUPFC as well as its optimal sizing and placement have been determined for cost and power loss reduction. A. Lashkar Ara *et al.* [23] applied the CONOPT solver to assign the locations and rating of the OUPFC under N-1 contingency for active power loss reduction. The optimal parameters setting OUPFC has been determined for transient stability of the system [24]. The placement and rating of the OUPFC has been assigned for power loss reduction and line collapse proximity indicator [25].

Enforcement the operating constrains is based on alleviating the specified values which are controlled by the FACTS. Then, the NR power flow is recomputed with the new alleviated values. It should be highlighted here that handling the constraints at their maximum values to maximize the utilization of the used controller.

The OUPFC is an efficient controller consists of a phase shifting transformer combined with a UPFC [22], [23], [24], [25]. Thus, the OUPFC is a combined series shunt controller, and it has ability to control the active and reactive power flow in TL. Few references have been presented to model or study the performance of the system with incorporating the OUPFC where the authors in [22] presented a power injection model of the OUPFC in steady state. In addition of that the proposed model has been applied on IEEE 14, 30, and 118-bus systems. However, the proposed model is an efficient model, but the shortages of the presented model are the operating constraints have not considered in load flow solution and the resistance of TL is ignored where only the TL reactance plus the injecting transformer reactance are augmented as one reactance and the load flow convergence characteristics of the presented model have not been presented. In [23], the optimal rating and placement of the OUPFC have been assigned using a Non-Linear Programming under a single line contingency. P. Avaz Pour *et al.* determined the parameters of the OUPFC for the transient stability enhancement [24]. The authors in [25] determined the optimal rating and location of the OUPFC using the cuckoo search algorithm for the power losses reduction and enhancing the system security.

B. CONTRIBUTION OF PAPER

In fact, the main contributions of this paper are (1) presenting an efficient novel model of the OUPFC into NR power flow, (2) avoiding the complicities of modeling the parameters of the OUPFC into power flow solution, (3) multi-control modes of the OUPFC are established to control the active and reactive powers concurrently or separately and, (4) handling the violation of the operating constraints by using developed methods. The proposed model is based on the power injection representation where the parameters of the OUPFC are represented as injected loads as a function of the pre-requested control variables (specified values). Therefore, the complicities of including its parameters are reduced. The developed methods for handling the violations of the operating constraints are based on modifying the specified values as a function of the maximum limits of the operating constraints.

C. PAPER LAYOUT

The paper is organized as follows: Section II 'Problem Formulation' described the NR method and inclusion of FACTS devices. Section III 'simulation results' shows the yielded results by application the OUPFC. Finally, Section IV 'Conclusion' summarizes the outcomes of the paper.

II. PROBLEM FORMULATION

A. NEWTON RAPHSON WITH INCLUSION OF FACTS DEVICES

Newton Raphson method is an efficient method that have been applied for solving power flow for an electrical system. Furthermore, it can be applied for solving the ill conditions and large-scale systems [26]. Generally, the Newton Raphson method for the power flow solution is expressed as follows:

$$[J][X] = [B] \tag{1}$$

where, J is the Jacobian matrix, X is the corrections matrix and B mismatches matrix. The NR matrices are

given as follows:

$$[J] = \begin{bmatrix} \frac{\partial P_2}{\partial \delta_2} & \cdots & \frac{\partial P_2}{\partial \delta_i} & \frac{\partial P_2}{\partial |V_2|} & \cdots & \frac{\partial P_2}{\partial |V_i|} \\ \vdots & \ddots & \vdots & \vdots & \ddots & \vdots \\ \frac{\partial P_i}{\partial \delta_2} & \cdots & \frac{\partial P_i}{\partial \delta_i} & \frac{\partial P_i}{\partial |V_2|} & \cdots & \frac{\partial P_i}{\partial |V_i|} \\ \frac{\partial Q_2}{\partial \delta_2} & \cdots & \frac{\partial Q_2}{\partial \delta_i} & \frac{\partial Q_2}{\partial |V_2|} & \cdots & \frac{\partial Q_2}{\partial |V_i|} \\ \vdots & \ddots & \vdots & \vdots & \ddots & \vdots \\ \frac{\partial Q_i}{\partial \delta_2} & \cdots & \frac{\partial Q_i}{\partial \delta_i} & \frac{\partial Q_i}{\partial |V_2|} & \cdots & \frac{\partial Q_i}{\partial |V_i|} \end{bmatrix} \quad (2)$$

$$[X] = \begin{bmatrix} \Delta\delta_2 \\ \vdots \\ \Delta\delta_i \\ \Delta\,|V_2| \\ \vdots \\ \Delta\,|V_i| \end{bmatrix} \quad (3)$$

$$[B] = \begin{bmatrix} \Delta P_2 \\ \vdots \\ \Delta P_n \\ \Delta Q_2 \\ \vdots \\ \Delta Q_n \end{bmatrix} \quad (4)$$

It should be highlighted here, in case of modeling the variable impedance-based FACTS devices, it requires a modification in Y matrix only or in bus and line data. The parameters of FACTS devices are considered as state variables in the Jacobian matrix, the corrections matrix mismatches matrix of the NR power flow solution as follows:

$$\begin{bmatrix} J & \\ & J_b \end{bmatrix} \begin{bmatrix} X \\ X_b \end{bmatrix} = \begin{bmatrix} B \\ B_b \end{bmatrix} \quad (5)$$

where, J_b, X_b and B_b are submatrices related to FACTS parameters.

B. OUPFC MODELLING AND OPERATING PRINCIPLE

The OUPFC is a developed controller that consists of PST and UPFC. The PST is tied with the secondary windings of a coupling transformer while UPFC involves of two voltage source converters couples with tertiary windings of a coupling transformer as depicted in Fig. 3. The PST injects a controllable AC voltage to the TL for changing the transmission angle. The UPFC's series converter is utilized for injecting an AC controllable voltage in series to the TL to adjust the power flow in this line while the shunt converter provides the active power demanded using the second or the series converter [22].

C. MODELING OF THE OUPFC INTO NR POWER FLOW

The OUPFC is a combined series-shunt controller injects an adjustable AC voltage in series with transmission line for control the powers flow through TL. Referring to Fig. 3,

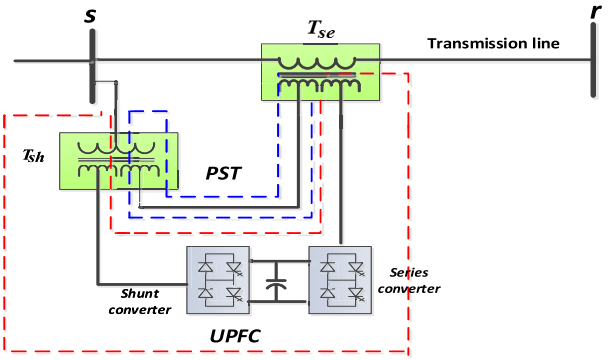

FIGURE 3. The construction of the OUPFC.

the OUPFC is connected between (s, r) buses where, s denotes the sending bus while r denotes the receiving bus. The equivalent circuit of the OUPFC includes a voltage source (V_{inj}) tied with the coupling transformer impedance (Z_s) and a shunt current source (I_{sh}) at the sending bus as depicted in Fig. 4 converter [22]. The auxiliary bus (j) is included at the terminal of the controller to assign the output power direction from this controller. Conventionally for modelling the OUPFC, the four state variables which are associated with the OUPFC (V_{inj}, θ_{inj}, V_{inj}, I_{sh} and θ_{sh}) should be added into the power flow solution. Thus, modeling of the OUPFC traditionally needs difficult modifications.

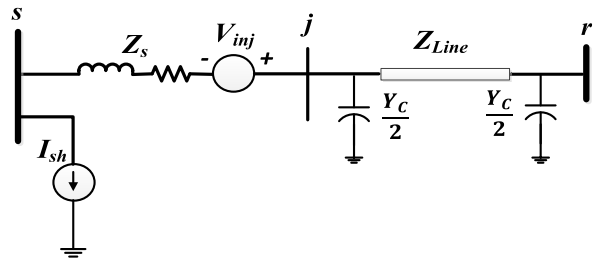

FIGURE 4. The injected current- voltage representation of the OUPFC [22].

The proposed model of the OUPFC is based on transforming the voltage source (V_{inj}) to current source which is shunted with of coupling transformer's impedance as depicted in Fig. 5. The value of the current is obtained using (6):

$$\overline{I_{inj}} = \frac{\overline{V_{inj}}}{\overline{Z_s}} \quad (6)$$

This current is calculated as a function of the specified active power and reactive power of the TL using Kirchhoff current law's at bus j as follows:

$$\overline{I_{inj}} = \overline{I_{sp}} - \overline{I_j} = \left(\frac{\overline{S_{sp}}}{\overline{V_j}}\right)^* - \left(\frac{\overline{V_s} - \overline{V_j}}{\overline{Z_s}}\right) \quad (7)$$

where, $\overline{S_{sp}} = P_{sp} + jQ_{sp}$ and $\overline{I_{sp}} = \overline{I_{jr}} + \overline{I_{c1}} + \overline{I_{c2}}$

It should be pointed out here that I_{sp} represents the current flow through the TL which can be assigned based on as the

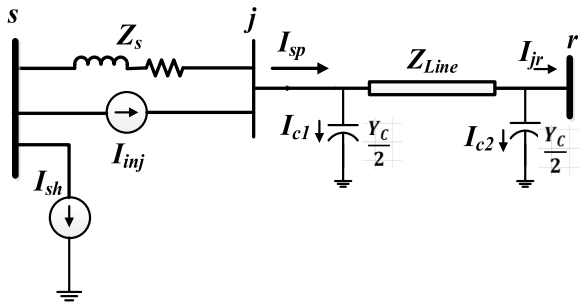

FIGURE 5. The current source representation of the OUPFC.

specified values (P_{sp}, Q_{sp}). The OUPFC does not exchange any powers with the system converter [22]. Hence,

$$3\overline{V_{inj}}\left(\overline{I_{sp}^{*}}\right) = 3\overline{V_s}\left(\overline{I_{sh}^{*}}\right) \tag{8}$$

It should be highlighted here that, Eq. (8) described the balanced apperaent power in the OUPFC where the left part of this equation refers to the injected power to the shunt converter while the right part refers to the injected power by the series converter. The exchanged real power in converters in a single phase is give as follows:

$$P_{ex} = Real\left(\overline{V_{inj}}\left(\overline{I_{sp}^{*}}\right)\right) = Re\left(\overline{V_s}\left(\overline{I_{sh}^{*}}\right)\right) \tag{9}$$

From (8) the shunt current is given as follows:

$$\overline{I_{sh}} = \left(\frac{\overline{V_{inj}}\left(\overline{I_{sp}^{*}}\right)}{\overline{V_s}}\right)^{*} \tag{10}$$

The proposed power injection model can be obtained by converting the current source I_{inj} into two injected shunt currents as shown in Fig. 6.

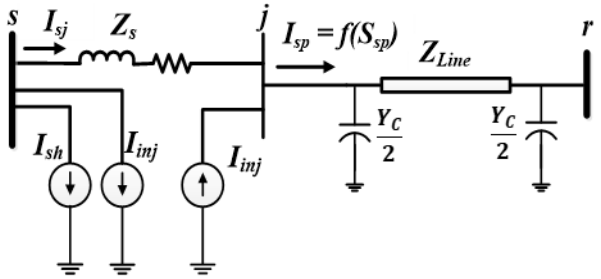

FIGURE 6. The shunt injected current sources representation of the OUPFC.

The shunt currents are converted to injected complex loads as presented in Fig. 7 using the following equations:

$$\overline{S_{sh}} = \overline{V_s}\left(\overline{I_{sh}^{*}}\right) \tag{11}$$

$$\overline{S_s} = \overline{V_s}\left(\overline{I_{inj}^{*}}\right) \tag{12}$$

$$\overline{S_j} = \overline{V_j}\left(-\overline{I_{inj}^{*}}\right) \tag{13}$$

It should be highlighted here that from the aforementioned equations, $\overline{V_{inj}}$ and $\overline{I_{sh}}$ are exchanged by injected loads which

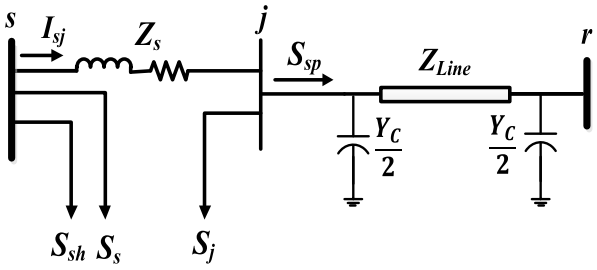

FIGURE 7. The proposed model of the OUPFC.

are updated as a function of the specified values, thus these values are avoided to be incorporated as state variables into load flow solution methods consequently, the complexities of modelling this controller are reduced.

D. THE CONTROL MODES OF THE OUPFC

The proposed OUPFC model is a resilience model where it can operate at different control modes as follows:

1) P-Q CONTROL MODE

In the P-Q or the full control mode, the OUPFC is adjusted to control the active power and the reactive power flow concurrently as:

$$P_{jr} - P_{sp} = 0 \tag{14}$$

$$Q_{jr} - Q_{sp} = 0 \tag{15}$$

2) P CONTROL MODE

The OUPFC is adjusted in this mode to control the active power flow only according to (16) while the reactive power is released.

$$P_{jr} - P_{sp} = 0 \tag{16}$$

The reactive power flow can be assigned as follows

$$Q_{jr} = Im\left(V_j\left(I_{jr}\right)^{*}\right) \tag{17}$$

$$I_{jr} = \frac{Y_c}{2}\left(V_j\right) + Y_{jr}\left(V_j - V_r\right) \tag{18}$$

3) Q CONTROL MODE

The OUPFC is adjusted in this mode to control the reactive power flow only according to (19).

$$Q_{jr} - Q_{sp} = 0 \tag{19}$$

The active power flow is uncontrolled value which can be found using (20).

$$P_{jr} = Real\left(V_j\left(I_{jr}\right)^{*}\right) \tag{20}$$

The steps of modeling the OUPFC into NR power flow are depicted in Fig. 8.

E. THE CONSTRAINTS ENFORCEMENT OF THE OUPFC

The constraints enforcement of the controllers is an important issue to assign the practical capability of these devices which

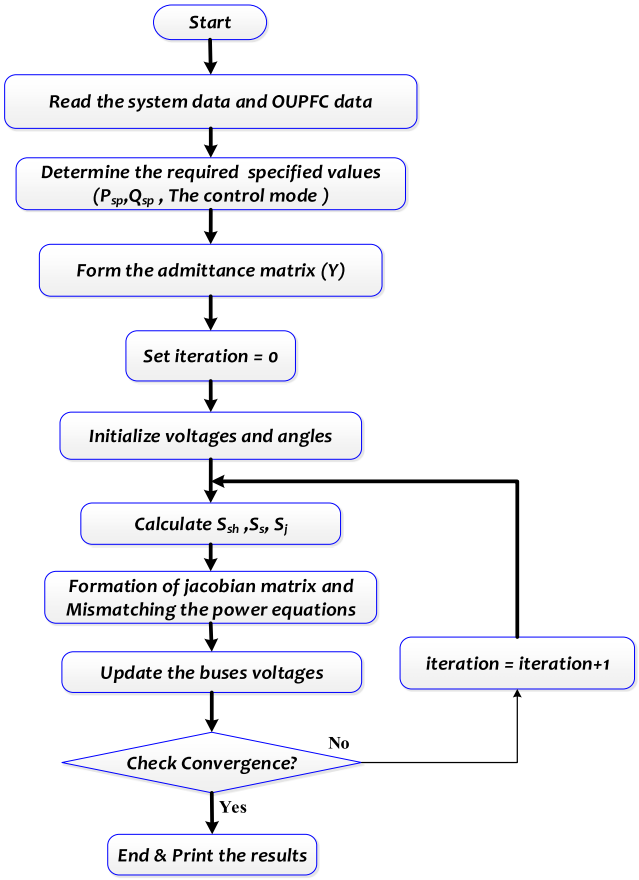

FIGURE 8. Flow chart for solving NR with load flow OUPFC model.

means determination or handling violations of the operating parameters of these controllers. The OUPF's operating constraints include the current passing through the OUPFC, the injected voltage, the shunt current and the real exchanged power. The operating constraints is enforced by minimizing the specified values at their maximum limits as the follows

- The passing current constraint via the OUPFC.

$$\left|I_{sp}\right| \leq I_{sp}^{max} \tag{21}$$

- The injected voltage constraint.

$$\left|V_{inj}\right| \leq V_{inj}^{max} \tag{22}$$

- The shunt current constraint.

$$|I_{sh}| \leq I_{sh}^{max} \tag{23}$$

- The exchanged power constraint.

$$P_{ex} \leq P_{ex}^{max} \tag{24}$$

The operating constraints can be enforced by two methods the first method is the conventional method which is based on minimizing the specified values gradually until the parameters be equal or less than their maximum limits as illustrated before. This method is simple to be applied but the main shortages of this method are low accuracy and the required simulation time is high due to the power flow repetition with the new minimized specified values. The proposed developed method is working on updating the specified parameters in the iterative NR power flow process as a function of the maximum limits which driven from equations of the mathematical representation of the presented model. Thus, the NR power flow will be repeated for one more time only. Consequently, the computation time will be reduced considerably compared to the conventional method. The constraints handling strategies are specified as follows

1) THE ENFORCEMENT OF THE SERIES CURRENT VIOLATION

There are two methods to adjusting series current at its maximum limit

a) Conventional method:
- Reducing P_{sp} gradually until I_{sp} equals or less than I_{sp}^{max} as depicted in (21)
- Reducing Q_{sp} gradually until I_{sp} equals or less than I_{sp}^{max} as depicted in (21)

b) Developed method

The specified active and reactive power are represented as a function of the maximum value of the series current and updated in the iterative process of the power flow. The modified specified values can be calculated as follows:

$$\overline{I_{sp}} = \left(\frac{\overline{S_{sp}}}{\overline{V_j}}\right)^* \tag{25}$$

$$I_{sp} - I_{sp}^{max} = 0 \tag{26}$$

$$I_{sp}^{max} = \left(\frac{P_{sp} + jQ_{sp}}{\overline{V_j}}\right)^* = \frac{P_{sp} - jQ_{sp}}{V_j^*} \tag{27}$$

$$\left|I_{sp}^{max}\right| = \frac{\sqrt{(P_{sp})^2 + (Q_{sp})^2}}{\sqrt{(V_j^{Re})^2 + (V_j^{Im})^2}} \tag{28}$$

where,

$$V_j = V_j^{Re} + V_j^{Im} \tag{29}$$

$$P_{sp} = \pm\sqrt{\left|I_{sp}^{max}\right|^2 \left((V_j^{Re})^2 + (V_j^{Im})^2\right) - Q_{sp}^2} \tag{30}$$

$$Q_{sp} = \pm\sqrt{\left|I_{sp}^{max}\right|^2 \left((V_j^{Re})^2 + (V_j^{Im})^2\right) - P_{sp}^2} \tag{31}$$

Eqs. (30) and (31) can be rewritten as follows

$$P_{sp}^{new} = \pm\sqrt{\left|I_{sp}^{max}\right|^2 \xi - Q_{sp}^2} \tag{32}$$

$$Q_{sp}^{new} = \pm\sqrt{\left|I_{sp}^{max}\right|^2 \xi - P_{sp}^2} \tag{33}$$

where, $\xi = (V_j^{Re})^2 + (V_j^{Im})^2$

It should be higlite here that the constraints of the OUPFC is handled at their maximum limits to maximizing the utilization of the OUPFC. However, the maximum value is varied with $\overline{V_j}$ but the specified value also changed to ensure that this value is at its maximum value with the iteration process of the load flow as depicted in (30) and (31).

2) ENFORCEMENT THE INJECTED VOLTAGE CONSTRAINT

If V_{inj} is violated, it should be enforced at its maximum allowable limit (V_{inj}^{max}). There are two methods to adjusting V_{inj} at its maximum limit:

a) Conventional method
- Reducing P_{sp} gradually until V_{inj} equals or less than V_{inj}^{max} until Eq. (22) is satisfied.
- Reducing Q_{sp} gradually until V_{inj} equals or less than V_{inj}^{max} until Eq. (22) is satisfied.

b) Developed method

The developed method is based on releasing the P_{sp} or the Q_{sp} as a function of V_{inj}^{max}. The new specified values can enforce V_{inj} to its V_{inj}^{max} and it can be assigned from (6) according to the following equations:

$$\overline{V}_{inj} = \overline{I}_{inj} \times \overline{Z}_s \tag{34}$$

By substituting I_inj from (8) in (35)

$$\overline{V}_{inj} = \left(\left(\frac{\overline{S_{sp}}}{\overline{V_j}}\right)^* - \left(\frac{\overline{V_s} - \overline{V_j}}{\overline{Z_s}}\right)\right)\overline{Z}_s \tag{35}$$

hence,

$$\overline{V}_{inj} = \frac{\left(\overline{S_{sp}}\right)^* \overline{Z}_s - \overline{V}_j^* \overline{V}_s + \overline{V}_j^* \overline{V}_j}{\overline{V}_j^*} \tag{36}$$

By substituting V_s, V_j, Z_s and S_{sp} in (36). Thereby, Eq. (36) is expressed as follows:

$$\overline{V}_{inj} = \frac{\begin{array}{l}\left(Q_{sp}X_s - \left(V_j^{Re}V_s^{Re} + V_j^{Im}V_s^{Im}\right) + \left((V_j^{Re})^2 + (V_j^{Im})^2\right)\right) \\ +j\left(\left(X_sP_{sp}\right) - \left(V_j^{Re}V_s^{Im} - V_j^{Im}V_s^{Re}\right)\right)\end{array}}{\overline{V}_j^*} \tag{37}$$

where,

$$V_s = V_s^{Re} + jV_s^{Im}, \quad V_j = V_j^{Re} + V_j^{Im}, \quad \xi = V_k^* V_k = (V_j^{Re})^2 + (V_j^{Im})^2, \quad Z_s = jX_s$$

Eq. (37) can be simplified as:

$$\overline{V}_{inj} = \frac{\left(Q_{sp}X_{se} - \lambda + \xi\right) + j\left(\left(X_{se}P_{sp}\right) - \beta\right)}{\overline{V}_j^*} \tag{38}$$

where,

$$\lambda = \left(V_j^{Re}V_s^{Re} + V_j^{Im}V_s^{Im}\right), \quad \beta = \left(V_j^{Re}V_s^{Im} - V_j^{Im}V_s^{Re}\right)$$

By substituting V_{inj} by V_{inj}^{max} in (38), the absolute value of V_{inj} can be given as:

$$\left|V_{inj}^{max}\right| = \frac{\left|\left(Q_{sp}X_s - \lambda + \xi\right) + j\left(\left(X_sP_{sp}^{new}\right) - \beta\right)\right|}{\left|\overline{V}_j^*\right|} \tag{39}$$

With doing some manipulations in (39), it can be rewritten as:

$$\left|V_{inj}^{max}\right|^2 \left|\overline{V}_j^*\right|^2 = \left(Q_{sp}X_s + \tau\right)^2 + \left(\left(X_sP_{sp}^{new}\right) - \beta\right)^2 \tag{40}$$

where, $\tau = -\lambda + \xi$. Eq. (40) can be reformulated as follows:

$$\left(X_sP_{sp}^{new}\right)^2 - 2\beta X_sP_{sp}^{new} + \left(Q_{sp}X_s\right)^2 + \tau^2 + 2X_s\tau Q_{sp} + \beta^2 - \left|V_{inj}^{max}\right|^2 \left|\overline{V}_j^*\right|^2 = 0 \tag{41}$$

This equation is a quadratic function. Therefore, it can be solved as follows:

$$P_{new}^{sp} = \frac{-B \pm \sqrt{B^2 - 4AC}}{2A} \tag{42}$$

where, $A = (X_s)^2$, $B = -2\beta X_s$ and $C = (X_s)^2\left(Q_{sp}\right)^2 + \tau^2 + 2Q_{sp}X_s\tau + \beta^2 - \left|V_{inj}^{max}\right|^2 \left|\overline{V}_j^*\right|^2$

By the same way, Q_{new}^{sp} that can handle violation of V_{inj} is calculated as follows:

$$Q_{new}^{sp} = \frac{-B \pm \sqrt{B^2 - 4AC}}{2A} \tag{43}$$

where, $A = (X_s)^2$, $B = 2X_s\tau$ *and* $C = (X_s)^2\left(P_{sp}\right)^2 - 2\beta X_sP_{sp} + \tau^2 + \beta^2 - \left|V_{inj}^{max}\right|^2 \left|\overline{V}_j^*\right|^2$

3) CONSTRAINT VIOLATION HANDLING OF THE SHUNT CURRENT

If I_{sh} is violated, it should be enforced at its maximum limit (I_{sh}^{max}) as follows
- Reducing P_{sp} gradually until $|I_{sh}|$ equals or less than I_{sh}^{max} until Eq. (23) is satisfied.
- Reducing Q_{sp} gradually until $|I_{sh}|$ equals or less than V_{inj}^{max} until Eq. (23) is satisfied.

4) CONSTRAINT VIOLATION HANDLING OF THE EXCHANGED POWER

If P_{ex} is violated, it should be enforced at the maximum limit (P_{ex}^{max}). There are two methods to adjusting P_{ex} at its maximum limit:

a) Conventional method
- Reducing P_{sp} gradually until P_{ex} equals or less than P_{ex}^{max} until Eq. (24) is satisfied.
- Reducing Q_{sp} gradually until P_{ex} equals or less than P_{ex}^{max} until Eq. (24) is satisfied.

b) Developed method

The developed method is based on releasing P_{sp} or Q_{sp} as a function of P_{ex}^{max}. The specified values that handle the exchanged power can be founded by Substituting the values of $\overline{V_{inj}}$ and I_{sp} from (38) and (25) in (9) as:

$$P_{ex} = Real\left(\left(\frac{\left(Q_{sp}X_{se} - \lambda + \xi\right) + j\left(\left(X_{se}P_{sp}\right) - \beta\right)}{\overline{V}_j^*}\right)\left(\frac{\overline{S_{sp}}}{\overline{V_j}}\right)\right) \tag{44}$$

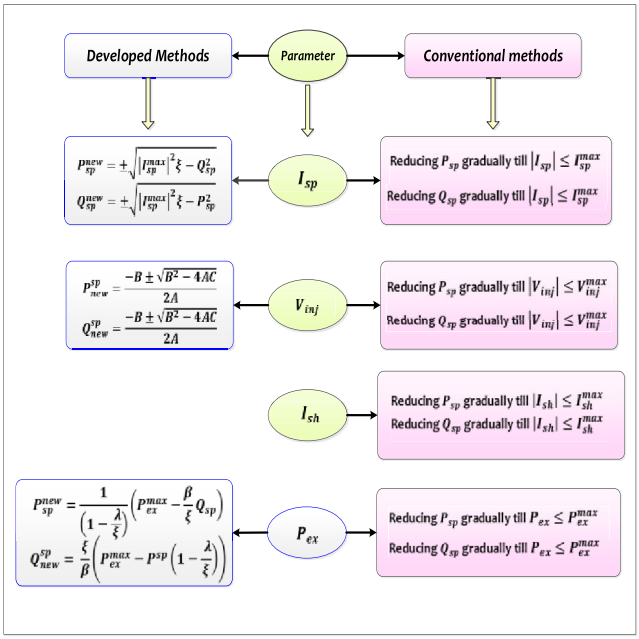

FIGURE 9. Constraints enforcement methods of the OUPFC.

By substituting $\overline{S_{sp}}$ in (44) and doing some manipulations. It can be formulated as follows:

$$P_{ex} = P_{sp}\left(1 - \frac{\lambda}{\xi}\right) + \frac{\beta}{\xi}Q_{sp} \tag{45}$$

From (45), the specified active power and the reactive power that enforce the exchanged power at its maximum limit are given as follows:

$$P_{sp}^{new} = \frac{1}{\left(1 - \frac{\lambda}{\xi}\right)}\left(P_{ex}^{max} - \frac{\beta}{\xi}Q_{sp}\right) \tag{46}$$

$$Q_{new}^{sp} = \frac{\xi}{\beta}\left(P_{ex}^{max} - P^{sp}\left(1 - \frac{\lambda}{\xi}\right)\right) \tag{47}$$

Fig. 9 depicts the handling constraints violation methods. Finally, Table 1 summarized all equations which have been used for modeling the proposed OUPFC.

III. SIMULATION RESULTS

The proposed model of the OUPFC into NR power flow as well as the operating constraints enforcement methods are validated and tested on IEEE 14-bus, IEEE 30-bus, IEEE 57-bus systems and IEEE 118-bus system in this section.

The line data and the bus data of the used IEEE 14-bus, IEEE 30-bus, IEEE 57-bus and IEEE 118-bus are given in [27]. The tolerance of the NR power flow is 10-5 and the MVA base is 100. The proposed model was written using MATLAB software (MATLAB 2018b) and carried out on a core i5 core PC with processor 2.50 GHz and 4 GB RAM. The studies cases are listed as flows:

A. IEEE14-BUS SYSTEM

Here, the OUPFC is inserted at line (6-13). It should be highlight here that the OUPFC can be inserted at any location and this location is arbitrary selected only for demonstrating the validity of the proposed model. The base power flow in this TL without inclusion OUPFC is 17.799 MW + j 7.461 MVAR. Tables 2 and 3 show the simulation results which obtained by inclusion of OUPFC. Five studied cases are presented with different specified values under full control mode as follows:

Case 1: In this case, the selected specified active and reactive powers (P_{sp}, Q_{sp}) that adjusted by OUPFC are 10 MW and 12 MVAR. The specified values are controlled to be less than the base case.

Case 2: In this case, the P_{sp} and Q_{sp} are selected to be 25 MW and 8 MVAR which are selected to be more than the powers in the base case.

Case 3: In this case, the P_{sp} and Q_{sp} are adjusted by OUPFC to be −20 MW and 10 MVAR. The specified active power is adjusted to be more than and in opposite direction of the base active power flow.

Case 4: In this case, the P_{sp} and Q_{sp} are adjusted by OUPFC to be −15 MW and −7 MVAR. The specified active and reactive power is adjusted to be in opposite direction of the base active and reactive powers flow.

Case 5: In this case, the P_{sp} and Q_{sp} are adjusted by OUPFC to be 20 MW and −7 MVAR. The specified active power is adjusted to be more than the base active power in the same direction while the specified reactive power is adjusted to be in opposite direction of the base reactive power flow.

According to Tables 2 and 3, the parameters of the OUPFC ($\overline{V_{inj}}$, $\overline{I_{sh}}$ and P_{ex}), the injected complex loads ($\overline{S_i}$, $\overline{S_k}$, $\overline{S_{sh}}$) and the voltage at the auxiliary bus j are changed with variations of the specified values. Judging from the aforementioned tables, the presented model is flexible to adjust the specified values to be more or less than the original powers flow. In addition to that it can adjust the directions of the power flow. Fig. 10 shows the absolute power mismatches of the NR power flow versus the iteration number with inclusion the proposed model for the previous cases. According to Fig. 10, it is clear the proposed model has stable and well convergences characteristics. It should be highlighted here that the power flow with inclusion the OUPFC using the proposed method is converged in 10 to 11 iterations while the convergance of the power flow with the conventional method [22] is not reported.

B. IEEE 30-BUS SYSTEM

Here, two OUPFC devices are installed in IEEE30-bus to demonstrates the efficacy and validity of the proposed model. Three studied cases are presented where two OUPFCs are embedded in system with different control modes (P-Q, P, Q) as well as different specified values and locations. Table 4 indicates the simulation results for the presented cases. In the first case, the OUPFC devices are incorporated in lines 5-7 and 2-4 and the OUPFCs work in full control modes. In the second case study, the OUPFC devices are incorporated in lines 2-6 and 9-10, both of the OUPFCs work under P

TABLE 1. Summarization of the used equations for modeling the OUPFC.

Modeling of the OUPFC	Control modes of the OUPFC
1) The injected loads for representation of the OUPFC	***1) P-Q Control Mode***
- $\overline{S_{sh}} = \overline{V_s}\left(\overline{I_{sh}^*}\right)$	- $P_{jr} - P_{sp} = 0$
- $\overline{S_s} = \overline{V_s}\left(\overline{I_{inj}^*}\right)$	- $Q_{jr} - Q_{sp} = 0$
- $\overline{S_j} = \overline{V_j}\left(-\overline{I_{inj}^*}\right)$	***2) P Control Mode***
2) The specified values	- $P_{jr} - P_{sp} = 0$
- $\overline{S_{sp}} = P_{sp} + jQ_{sp}$	- $Q_{jr} = Im\left(V_j\left(I_{jr}\right)^*\right)$
3) The shunt injected current.	***3) Q Control Mode***
- $\overline{I_{sh}} = \left(\frac{\overline{V_{inj}}\left(\overline{I_{sp}^*}\right)}{\overline{V_s}}\right)^*$	- $Q_{jr} - Q_{sp} = 0$
4) The exchanged power	- $P_{jr} = Real\left(V_j\left(I_{jr}\right)^*\right)$
$P_{ex} = Real\left(\overline{V_{inj}}\left(\overline{I_{sp}^*}\right)\right) = Re\left(\overline{V_s}\left(\overline{I_{sh}^*}\right)\right)$	
Methods of the constraints enforcement	
1) I_{sp}	***2) V_{inj}***
a) Conventional method	***a) Conventional method***
- Reducing P_{sp} gradually until I_{sp} equals or less than I_{sp}^{max}.	- Reducing P_{sp} gradually until V_{inj} equals or less than V_{inj}^{max} .
- Reducing Q_{sp} gradually until I_{sp} equals or less than I_{sp}^{max} .	- Reducing Q_{sp} gradually until V_{inj}equals or less than V_{inj}^{max}.
b) Developed method	***a) Developed method***
- $P_{sp}^{new} = \pm\sqrt{\left\|I_{sp}^{max}\right\|^2\xi - Q_{sp}^2}$	- $\boldsymbol{P_{new}^{sp}} = \frac{-B\pm\sqrt{B^2-4AC}}{2A}$
- $Q_{sp}^{new} = \pm\sqrt{\left\|I_{sp}^{max}\right\|^2\xi - P_{sp}^2}$	- $Q_{new}^{sp} = \frac{-B\pm\sqrt{B^2-4AC}}{2A}$
3) I_{sh}	***4) P_{ex}***
a) Conventional method	***a) Conventional method***
- Reducing P_{sp} gradually until P_{ex} equals or less than P_{ex}^{max}.	- Reducing P_{sp} gradually until P_{ex} equals or less than P_{ex}^{max}.
- Reducing Q_{sp} gradually until P_{ex} equals or less than P_{ex}^{max}	- Reducing Q_{sp} gradually until P_{ex} equals or less than P_{ex}^{max}.
	b) Developed method
	- $\boldsymbol{P_{sp}^{new}} = \frac{1}{\left(1-\frac{\lambda}{\xi}\right)}\left(\boldsymbol{P_{ex}^{max}} - \frac{\beta}{\xi}\boldsymbol{Q_{sp}}\right)$
	- $\boldsymbol{Q_{new}^{sp}} = \frac{\xi}{\beta}\left(\boldsymbol{P_{ex}^{max}} - \boldsymbol{P^{sp}}\left(1-\frac{\lambda}{\xi}\right)\right)$

TABLE 2. Parameters of the OUPFC with different specified values (IEEE 14-bus system).

Case	P_{sp} (MW)	Q_{sp} $(MVAr)$	$\overline{V_{inj}}(p.u)$	$\overline{I_{sh}}(p.u)$	$P_{ex}(MW)$	Simulation time (Sec.)
1	10	12	0.03626 ∠-87º	0.0049 ∠6º	0.49607	0.0628
2	25	8	0.05694 ∠51º	0.0128 ∠-96º	0.19085	0.04029
3	-20	10	0.20793 ∠-132º	0.0443 ∠-59º	3.35238	0.04471
4	-15	-7	0.20129 ∠-159º	0.0338 ∠-80º	1.47950	0.04562
5	20	-15	0.13872 ∠128º	0.03312 ∠-116º	-0.73169	0.048565

TABLE 3. The complex loads and the auxiliary voltage with inclusion of one OUPFC (IEEE 14-bus system).

Case	P_{sp} (MW)	Q_{sp} (MW)	$\overline{V_{aux}}(p.u)$	$\overline{S_i}(MVA)$	$\overline{S_k}(MVA)$	$\overline{S_{sh}}(MVA)$
1	10	12	1.070 ∠-16.37º	-37.09 +j11.36	36.60 -j12.86	0.488 - j0.205
2	25	8	1.087 ∠-12.92º	55.56 +j24.98	-55.75 -j26.86	0.157 +j 1.39
3	-20	10	0.980 ∠-23.25º	-196.66 -j1.040	193.31+ j64.17	3.535 + j2.53
4	-15	-7	0.919 ∠-20.12º	-122.6 -j177.08	121.13+ j139.8	1.570 + j2.69
5	20	-15	0.979 ∠-10.78º	90.18 - j117.90	-89.44 + j 102.1	-0.878 + j3.12

control modes while in this third case, the OUPFC devices are connected in lines 6-10 and 12-4. The first OUPFC operates at P control mode while the anther OUPFC operates under Q control mode. From Table 4, it obvious that the parameters of the OUPFCs follow the changes of the specified values and the control modes.

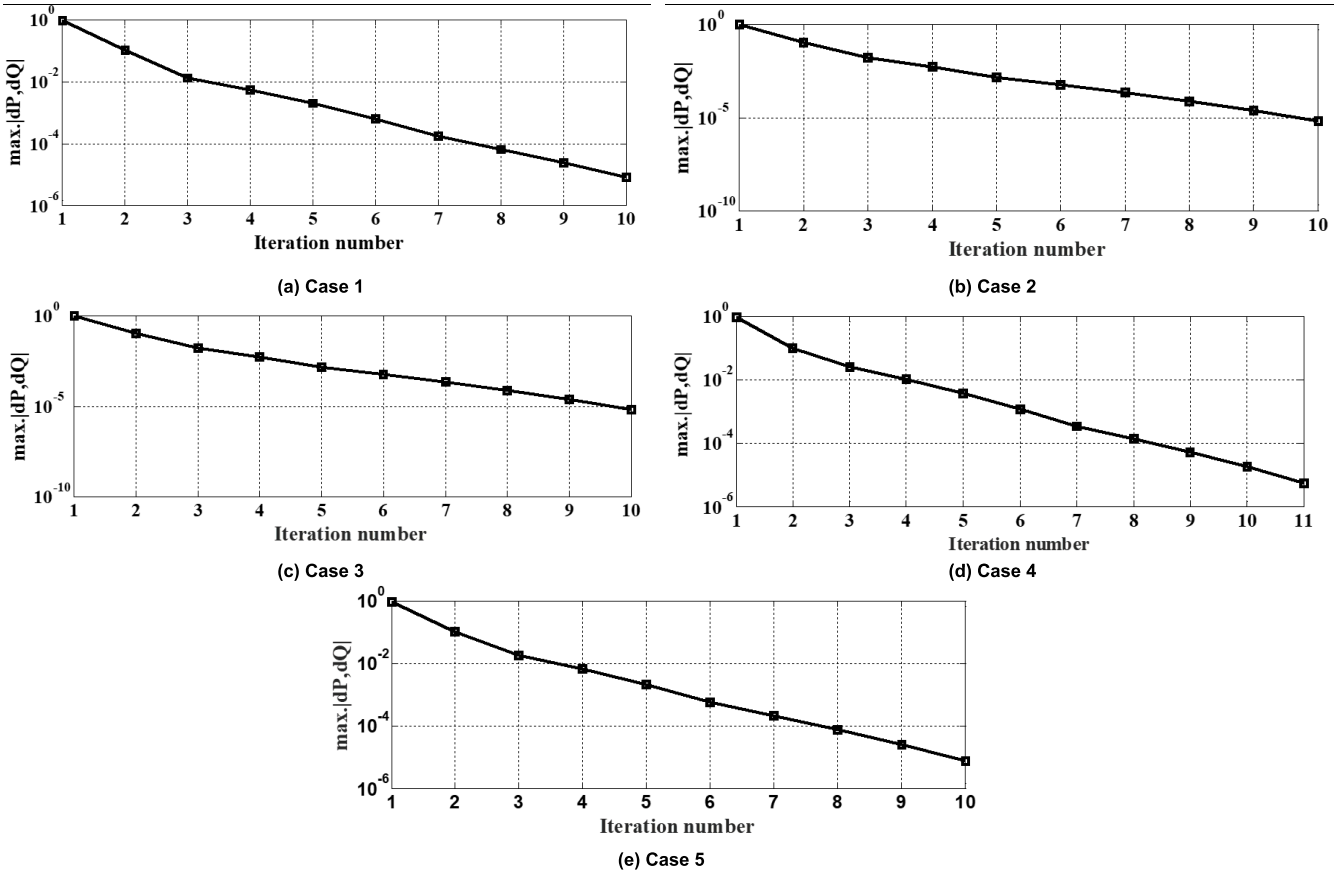

FIGURE 10. The convergence characteristic of NR power flow for (a) case 1, (b) case 2, (c) case 3, (d) case 4, (e) case 5.

TABLE 4. Simulation results for the IEEE 30-bus system with incorporating two OUPFCs.

Parameters	Case (1)		Case (2)		Case (3)	
Location	OUPFC1	OUPFC2	OUPFC1	OUPFC2	OUPFC1	OUPFC2
	5-7	2-4	2-6	9-10	6-10	12-4
Control mode	*P-Q*	*P-Q*	*P*	*P*	*P*	*Q*
Base P (MW)	-14.205	45.712	61.912	27.693	15.823	-44.121
Base Q (MVar)	10.500	2.705	-0.958	6.741	0.653	-9.961
P_{sp}(MW)	-15	50	65	30	20	-45
Q_{sp}(MVar)	15	5	-2	8	2	-15
$\overline{I_{sh}}(p.u)$	0.00612 ∠66º	0.02240 ∠85º	0.05933 ∠71º	0.00836 ∠72º	0.00045 ∠-134º	0.00459 ∠119º
$\overline{V_{inj}}(p.u)$	0.02969 ∠-50º	0.04884 ∠78º	0.09428 ∠111º	0.03041 ∠75º	0.00229 ∠-60º	0.02156 ∠165º
$\overline{S_t}(MVA)$	-17.35 +24.46	50.6633 +j 5.31	87.53 -j44.82	32.079+ j0.06	-1.7178 + j1.55	-2.36 –j22.52
$\overline{S_k}(MVA)$	17.45 -j24.74	-50.98 - j5.81	-86.14 +j41.96	-31.54 - j0.51	1.69 - j1.59	-1.34 +j20.96
$\overline{S_{sh}}(MVA)$	0.105-j0.62	-0.011 - j2.35	1.476 –j5.84	0.065-j0.86	-0.024 + j0.039	-0.291 – j0.34
$P_{ex}(MW)$	0.10517	-0.03227	1.39471	0.05370	-0.02464	-0.37083

C. IEEE 57-BUS SYSTEM

In this section the OUPFC constraints have been enforced by application the conventional and the proposed methods. the OUPFC is inserted at line (4-6). Without inclusion the OUPFC, the power flow in this line is 14.159 MW – j 5.095 MVar. The adjusted specified active and reactive powers by the OUPFC are 60 MW and 55 MVar, respectively. Table 5 list the studied cases. In Table 5, the bolded values refer to the enforced parameter and the corresponding modified specified values. The following cases describe application of the studied cases are summarized as follows:

Case (1): This case is the based case where the OUPFC is inserted in line 4-6 to adjust the active and reactive powers for this line to be 60 MW and 55 MVar, respectively. In this case, the constraints handling methods are not applied.

Case (2): In this case, the active and reactive powers are adjusted like case (1), except that I_{sp} is limited to be 0.6 p.u. I_{sp} is adjusted to it maximum limit (I_{sp}^{max}) using the developed

TABLE 5. Studied cases of the operating constraints handling methods (IEEE 57-bus).

Case	$P_{sp}(MW)$	$Q_{sp}(MVAR)$	$\lvert I_{sp}\rvert(p.u)$	$\lvert V_{inj}\rvert(p.u)$	$\lvert I_{sh}\rvert(p.u)$	$P_{ex}(MW)$	Simulation time (Sec.)
(1)	60	55	0.7346	0.2374	0.18210	4.77796	0.330
(2)	**36.5602**	55	**0.6000**	0.19458	0.12137	3.94373	0.588
(3)	**-33.4482**	55	**0.6000**	0.25802	0.15957	4.79961	0.543
(4)	**36.5100**	55	**0.5998**	0.20215	0.12720	4.40825	28.902
(5)	60	**21.9429**	**0.6000**	0.19028	0.11774	3.72068	0.626
(6)	60	**-6.1007**	**0.6000**	0.18109	0.11136	2.91307	0.687
(7)	60	**21.8800**	**0.5998**	0.19255	0.12018	4.26841	36.59
(8)	**29.3008**	55	0.5674	**0.19500**	0.11595	4.24200	0.519
(9)	**-8.1106**	55	0.5173	**0.19500**	0.10440	4.11784	0.817
(10)	**29.200**	55	0.5670	**0.19492**	0.11582	4.24013	26.885
(11)	60	**25.273**	0.6144	**0.19500**	0.12501	3.84583	0.720
(12)	60	**23.900**	0.6050	**0.19448**	0.12283	4.30772	25.505
(13)	**54.3550**	55	0.6990	0.23108	**0.16999**	5.11198	33.859
(14)	60	**48.2300**	**0.**7001	0.23104	**0.16999**	5.10625	29.097
(15)	**39.2309**	55	0.6133	0.19823	0.12645	**4.00000**	1.395
(16)	**39.2000**	55	0.6131	0.19819	0.12639	**3.99934**	10.549

method by adjusting P_{sp} according to (32). The new P_{sp} by application the first root of Eq. (32) is 36.5602 MW for handling I_{sp}. The simulation time for this case is 0.588 second.

Case (3): I_{sp} is adjusted to its maximum limit like case (2) but I_{sp} is adjusted using the developed method to it maximum limit (I_{sp}^{max}) by using the second root of Eq. (32). The required simulation time for this case is 0.543 second.

Case (4): I_{sp} is adjusted to it maximum limit (0.6 p.u) like case (2) but using the conventional method by minimizing P_{sp} gradually until (21) is satisfied. The new specified value by application this method is 36.5100 MW. This value adjusted $\boldsymbol{I_{sp}}$ to 0.5998 p.u. However, Eq. (21) is satisfied but it less than the required maximum limit value by 0.0002 p.u. Thus, the developed method is more accurate compared with the developed method (Cases 2 and 3) time as well as it needs more commotional time compared with developed method where the required simulation time is 28.902 second.

Case (5): I_{sp} is limited to be 0.6 p.u. I_{sp}^{max} using the developed method by adjusting Q_{sp} according to (33). The new reactive power by application the first root of Eq. (33) is 21.9429 MVar for handling I_{sp}. The required simulation time for this case is 0.626 second.

Case (6): I_{sp} is adjusted using the developed method to it maximum limit (I_{sp}^{max}) by application the second root of Eq. (33). The obtained specified reactive power is −6.1007 MVar. The required simulation time for this case is 0.687 second.

Case (7): I_{sp} is adjusted to it maximum limit 0.6 p.u using the conventional method by minimizing Q_{sp} gradually until (21) is satisfied. The new specified value by application this method is 21.88 MVar. This value adjusted I_{sp} to 0.5998 p.u. The required simulation time for this case is 36.59 second. Thus, this method needs more required simulation time and less accurate compared with the proposed develop methods cases (5, 6).

Case (8): This case this case (1), except that $\lvert V_{inj}\rvert$ is limited to be 0.195 p.u. $\lvert V_{inj}\rvert$ is adjusted to it maximum limit (V_{inj}^{max}) using the developed method by adjusting P_{sp} according to (42). The new P_{sp} by application the first root of Eq. (42) is 29.3008 MW for handling the violation of the $\lvert V_{inj}\rvert$. The required simulation time for this case is 0.519 second.

Case (9): This case is like case (8), except that $\lvert V_{inj}\rvert$ is enforced by modifying P_{sp} using the developed method by application the second root of Eq. (42). The new specified active power is −8.1106 MW and the required simulation time for this case is 0.817 second.

Case (10): This case like case (8), but $\lvert V_{inj}\rvert$ is adjusted to it maximum limit (0.195 p.u) using the conventional method by minimizing P_{sp} gradually until (22) is satisfied. The new specified value by application this method is 29.200 MW. This value adjusted $\lvert V_{inj}\rvert$ to 0.19492 p.u. However, Eq. (22) is satisfied but it less than the required maximum limit value (0.195 p.u). Thus, the developed method for this case is more accurate compared with the developed method (Cases 8 and 9) time as well as it needs more commotional time compared with developed method where the required simulation time is 26.885 second.

Case (11): This case is like case (8), where $\lvert V_{inj}\rvert$ is limited to V_{inj}^{max} using the developed method by adjusting Q_{sp} according to (43). The new reactive power by application of Eq. (43) is 25.273 MVar for handling V_{inj}. The required simulation time for this case is 0.720 second.

Case (12): This case is like case (5), where $\lvert V_{inj}\rvert$ is limited to V_{inj}^{max} but by using the conventional method by minimizing Q_{sp} gradually until (22) is satisfied. The new specified value by application this method is 23.900 MVar. This value adjusted $\lvert V_{inj}\rvert$ to 0.19448 p.u. The required simulation time for this case is 25.505 second. Thus, this method needs more required simulation time and less accurate compared with the proposed develop methods case 11.

Case (13): It is like case (1), except that I_{sh}^{max} is assumed to be 0.17 p.u. I_{sh} is enforced to its maximum limit by reducing P_{sp} gradually till Eq. (23) is satisfied. The new specified

TABLE 6. Simulation results for the IEEE 118-bus system with incorporating two OUPFCs.

Parameters	Case (1)		Case (2)	
Location	OUPFC1	OUPFC2	OUPFC1	OUPFC2
	19-34	37-33	65-68	91-92
Control mode	*P-Q*	*P-Q*	*P-Q*	*P-Q*
Base P (MW)	-2.600	14.784	61.912	19.984
Base Q (MVar)	-7.319	8.745	-0.958	-9.628
P_{sp}(MW)	10	10	25	30
Q_{sp}(MVar)	12	8	12	8
$\overline{V_{inj}}(p.u)$	0.17832 ∠47°	0.04109 ∠37°	0.18885 ∠92°	0.17907 ∠33°
$\overline{S_i}(MVA)$	17.25+j22.84	-3.06 - j6.03	28.78+j13.12	-27.024+j11.186
$\overline{S_k}(MVA)$	-17.49+j25.47	-3.06 - j6.04	-28.8 -j13.91	27.24 -j12.71
$\overline{S_{sh}}(MVA)$	-0.1389 - j2.9	-0.2375 - j0.47	0.104 - j5.21	0.047 - j3.94
$P_{ex}(MW)$	-0.24864	-0.22038	1.39471	0.21421

value is 54.3550 MW while the required simulation time is 33.859 second.

Case (14): It is like case (13), except that I_{sh} is enforced to its maximum limit (0.17 p.u) by reducing Q_{sp} gradually till Eq. (23) is satisfied. The new specified reactive power for this case is 48.23 MVar while the required simulation time is 29.097 second.

Case (15): In this case P_{ex}^{max} is assumed to be 4 MW. P_{ex} is adjusted to its maximum limit by modifying P_{sp} by application the developed method by application Eq. (46). The obtained g P_{sp} is 39.2309 MW and the required simulation time for this case 1.395 second.

Case (16): It is like case (15), but the P_{ex} is limited to its maximum limit (4 MW) conventionally by reducing P_{sp} gradually till Eq. (24) is satisfied. The new specified active power for this case is 39.20 MVar while the required simulation time is 10.549 second. the required simulation time of this method is more than the developed method (Case 15).

D. IEEE 118-BUS SYSTEM

In this section two OUPFCs with the proposed model are incorporated in 118-bus system as a large scale system for verifying the valaidity of the proposed algorithm. Two studied cases are presented.

Table 6 indicates the simulation results for the presented cases. In the first case, the OUPFC devices are incorporated in lines 19-34 and 37-33 and the OUPFCs work in full control modes. In the second case study, the OUPFC devices are incorporated in lines 65-68 and 91-92, both of the OUPFCs work under P-Q control modes. From Table 5, it obvious that the parameters of the OUPFCs follow the changes of the specified values and the control modes.

E. DISCUSSION

The simulation results reveal to that the proposed model is a flexible and feasibility model and it can work under different specified values as depicted in Table 2 and 3. Five studied have been presented in Table 2 and 3 under different specified values (P_{sp}, Q_{sp}) are selected to be more or less or in opposite direction of the power flow in base case (17.799 MW + j 7.461 MVAR). In addition of that the power flow with the proposed model is converged at the 10 to 11 iterations for the studied cases in the IEEE 14-bus system. The detailed implementation of such a multi-control functional model in power flow is presented. Two OUPFCs have been incorporated in the IEEE 30-bus system with different control modes which verified the effectiveness of this model. Judging from Table 5, The operating constraints in the presented model can be handled by several strategies with application the conventional and the proposed developed method.

The obtained results in the IEEE 57-bus system by application of the proposed developed methods of cases 2, 3, 5, 6, 8, 9, 11 and 15 are more precisely compared to those obtained by application the conventional methods of cases 4, 7, 10, and 12. For example in cas by e of handling the I_{sp} at 0.6 p.u., this value is enforced precisely at this value using the developed method in cases 2, 3, 5 and 6 while in case of application the conventional methods (cases 4 and 7) this value is less than 0.6 p.u. In addition, the developed methods need less computational time compared with the conventional method.

The obtained results in the 118-bus system, verify the effectiveness of the proposed model to be applied in large scale system.

IV. CONCLUSION

This paper presented a novel model of the OUPFC device into the Newton Raphson power flow solution. The proposed model is based on representing the OUPFC as active and reactive loads at the terminals of the controller. The complex modifications into Newton Raphson power flow for representing the OUPFC have been avoided due to exchanging the parameters of the OUPFC by the injected loads. In this model, the violation of the operating constraints has been addressed using conventional and developed methods. The developed methods are based on modification the specified values as a function of the maximum limits of the constraints. To verify the validity of the proposed model and the constraints enforcement method, they have been tested on IEEE 14-bus, 30-bus 57- bus, and 118-bus test systems. The simulation results reveal the following conclusions:

- The proposed model is a robust model, and it has a stable and rapid convergence characteristic.
- In the presented model, the OUPFC can operate in multi-control modes to control the active or reactive powers flow separately or simultaneously.
- The proposed developed methods for constraints enforcement are superior compared with the conventional methods in terms of the precision and the computational time.

REFERENCES

[1] B. Singh, R. P. Payasi, and V. Shukla, "A taxonomical review on impact assessment of optimally placed DGs and FACTS controllers in power systems," *Energy Rep.*, vol. 3, pp. 94–108, Nov. 2017.
[2] F. H. Gandoman, A. Ahmadi, A. M. Sharaf, P. Siano, J. Pou, B. Hredzak, and V. G. Agelidis, "Review of FACTS technologies and applications for power quality in smart grids with renewable energy systems," *Renew. Sustain. Energy Rev.*, vol. 82, pp. 502–514, Feb. 2018.
[3] K. Padiyar, *FACTS Controllers in Power Transmission and Distribution*. New Age International, 2007.
[4] X.-P. Zhang, C. Rehtanz, and B. Pal, *Flexible AC Transmission Systems: Modelling and Control*. Springer, 2012.
[5] S. Kamel, F. Jurado, and R. Mihalic, "Advanced modeling of center-node unified power flow controller in NR load flow algorithm," *Electr. Power Syst. Res.*, vol. 121, pp. 176–182, Apr. 2015.
[6] E. Acha, C. R. Fuerte-Esquivel, H. Ambriz-Perez, and C. Angeles-Camacho, *FACTS: Modelling and Simulation in Power Networks*. Hoboken, NJ, USA: Wiley, 2004.
[7] M. Noroozian, L. Angquist, M. Ghandhari, and G. Andersson, "Use of UPFC for optimal power flow control," *IEEE Trans. Power Del.*, vol. 12, no. 4, pp. 1629–1634, Oct. 1997.
[8] M. I. Alomoush, "Derivation of UPFC DC load flow model with examples of its use in restructured power systems," *IEEE Trans. Power Syst.*, vol. 18, no. 3, pp. 1173–1180, Aug. 2003.
[9] A. Nabavi-Niaki and M. R. Iravani, "Steady-state and dynamic models of unified power flow controller (UPFC) for power system studies," *IEEE Trans. Power Syst.*, vol. 11, no. 4, pp. 1937–1943, Nov. 1996.
[10] D. J. Gotham and G. T. Heydt, "Power flow control in systems with FACTS devices," *Electr. Mach. Power Syst.*, vol. 26, no. 9, pp. 951–962, Nov. 1998.
[11] M. H. Haque and C. M. Yam, "A simple method of solving the controlled load flow problem of a power system in the presence of UPFC," *Electr. Power Syst. Res.*, vol. 65, no. 1, pp. 55–62, Apr. 2003.
[12] C. R. Fuerte-Esquivel, E. Acha, and H. Ambriz-Perez, "A comprehensive Newton–Raphson UPFC model for the quadratic power flow solution of practical power networks," *IEEE Trans. Power Syst.*, vol. 15, no. 1, pp. 102–109, Feb. 2000.
[13] C. R. Fuerte-Esquivel and E. Acha, "Unified power flow controller: A critical comparison of Newton–Raphson UPFC algorithms in power flow studies," *Gener., Transmiss. Distrib.*, vol. 144, no. 5, pp. 437–444, Sep. 1997.
[14] S. Bhowmick, B. Das, and N. Kumar, "An indirect UPFC model to enhance reusability of Newton power-flow codes," *IEEE Trans. Power Del.*, vol. 23, no. 4, pp. 2079–2088, Oct. 2008.
[15] M. Ebeed, S. Kamel, and F. Jurado, "Determination of IPFC operating constraints in power flow analysis," *Int. J. Electr. Power Energy Syst.*, vol. 81, pp. 299–307, Oct. 2016.
[16] M. Ebeed, S. Kamel, and F. Jurado, "Constraints violation handling of GUPFC in Newton–Raphson power flow," *Electr. Power Compon. Syst.*, vol. 45, no. 9, pp. 925–936, May 2017.
[17] M. Ebeed, S. Kamel, and F. Jurado, "Constraints violation handling of SSSC with multi-control modes in Newton–Raphson load flow algorithm," *IEEJ Trans. Electr. Electron. Eng.*, vol. 12, no. 6, pp. 861–866, Nov. 2017.
[18] M. Ebeed, S. Kamel, J. Yu, and F. Jurado, "Development of UPFC operating constraints enforcement approach for power flow control," *IET Gener., Transmiss. Distrib.*, vol. 13, no. 20, pp. 4579–4591, Oct. 2019.
[19] S. Kamel, M. Ebeed, J. Yu, and W. Li, "A comprehensive model of C-UPFC with innovative constraint enforcement techniques in load flow analysis," *Int. J. Electr. Power Energy Syst.*, vol. 101, pp. 289–300, Oct. 2018.
[20] X.-P. Zhang, "Advanced modeling of the multicontrol functional static synchronous series compensator (SSSC) in Newton power flow," *IEEE Trans. Power Syst.*, vol. 18, no. 4, pp. 1410–1416, Nov. 2003.
[21] J.-Y. Liu, Y.-H. Song, and P. A. Mehta, "Strategies for handling UPFC constraints in steady-state power flow and voltage control," *IEEE Trans. Power Syst.*, vol. 15, no. 2, pp. 566–571, May 2000.
[22] A. L. Ara, A. Kazemi, and S. A. N. Niaki, "Modelling of optimal unified power flow controller (OUPFC) for optimal steady-state performance of power systems," *Energy Convers. Manage.*, vol. 52, no. 2, pp. 1325–1333, Feb. 2011.
[23] A. L. Ara, J. Aghaei, M. Alaleh, and H. Barati, "Contingency-based optimal placement of optimal unified power flow controller (OUPFC) in electrical energy transmission systems," *Scientia Iranica*, vol. 20, no. 3, pp. 778–785, 2013.
[24] P. A. Pour, A. L. Ara, and S. A. N. Niaki, "Enhancing power system transient stability using optimal unified power flow controller based on Lyapunov control strategy," *Scientia Iranica*, vol. 24, no. 3, pp. 1458–1466, Jun. 2017.
[25] K. V. K. Kavuturu and P. V. R. L. Narasimham, "Transmission security enhancement under (N−1) contingency conditions with optimal unified power flow controller and renewable energy sources generation," *J. Electr. Eng. Technol.*, vol. 15, no. 4, pp. 1617–1630, Jul. 2020.
[26] H. Saadat, *Power System Analysis*. New York, NY, USA: McGraw-Hill, 1999.
[27] *Power Systems Test Case Archive*. University of Washington, Seattle. [Online]. Available: https://www.ee.washington.edu/research/pstca/

MOHAMED EBEED HUSSEIN was born in Aswan, Egypt, in 1983. He received the B.S. degree from Aswan University, Egypt, in 2005, the M.S. degree in electrical engineering from South Valley University, in 2013, and the jointly-supervised Ph.D. degree from the Department of Electrical Engineering, Faculty of Engineering, Aswan University, and the University of Jaén, Spain, in 2018. From 2008 to 2009, he was a Lecturer at Aswan Technical Institute. From 2009 to 2017, he was a Maintenance Engineer at EFACO Company. He is currently an Assistant Professor with the Department of Electrical Engineering, Faculty of Engineering, Sohag University, Egypt.

FATMA RABEA received the B.Sc. degree from Aswan University, in 2016, where she is currently pursuing the M.Sc. degree with the Department of Electrical Engineering, Faculty of Engineering. Her research interests include power system modeling, analysis, and simulation, applications of power electronics to power systems, and power quality.

SALAH KAMEL received the International Ph.D. degree from the University of Jaén, Spain (Main), and Aalborg University, Denmark (Host), in January 2014. He is currently an Associate Professor with the Department of Electrical Engineering, Aswan University. He is also a Leader of the Advanced Power Systems Research Laboratory (APSR Lab), Power Systems Research Group, Aswan, Egypt. His research interests include power system analysis and optimization, smart grid, and renewable energy systems.

EYAD S. ODA (Member, IEEE) received the B.Sc. degree in electrical engineering from Suez Canal University, Egypt, in 2006, the M.Sc. degree in electrical engineering from Port Said University, Egypt, in 2012, and the Ph.D. degree in electrical engineering from Suez Canal University, in 2017. He is currently an Assistant Professor with Suez Canal University. His research interests include application of artificial intelligence and optimization algorithms in power systems.